BRAIN CONNECTIVITY
Volume 4, Number 7, 2014
© Mary Ann Liebert, Inc.
DOI: 10.1089/brain.2014.0254

Brainstem Stimulation Increases Functional Connectivity of Basal Forebrain-Paralimbic Network in Isoflurane-Anesthetized Rats

Siveshigan Pillay,[1] Xiping Liu,[1] Péter Baracskay,[2] and Anthony G. Hudetz[1]

Abstract

Brain states and cognitive-behavioral functions are precisely controlled by subcortical neuromodulatory networks. Manipulating key components of the ascending arousal system (AAS), via deep-brain stimulation, may help facilitate global arousal in anesthetized animals. Here we test the hypothesis that electrical stimulation of the oral part of the pontine reticular nucleus (PnO) under light isoflurane anesthesia, associated with loss of consciousness, leads to cortical desynchronization and specific changes in blood-oxygenation-level-dependent (BOLD) functional connectivity (FC) of the brain. BOLD signals were acquired simultaneously with frontal epidural electroencephalogram before and after PnO stimulation. Whole-brain FC was mapped using correlation analysis with seeds in major centers of the AAS. PnO stimulation produced cortical desynchronization, a decrease in δ- and θ-band power, and an increase in approximate entropy. Significant increases in FC after PnO stimulation occurred between the left nucleus Basalis of Meynert (NBM) as seed and numerous regions of the paralimbic network. Smaller increases in FC were present between the central medial thalamic nucleus and retrosplenium seeds and the left caudate putamen and NBM. The results suggest that, during light anesthesia, PnO stimulation preferentially modulates basal forebrain-paralimbic networks. We speculate that this may be a reflection of disconnected awareness.

Key words: ascending arousal system; consciousness; functional connectivity magnetic resonance imaging (fcMRI); anesthesia

Introduction

Communication among discrete neural regions and networks is fundamental to conscious perception, behavior, learning, memory, and cognition (Bressler and Menon, 2010; Sporns, 2014). The flow of information among remote brain regions is under the control of elaborate subcortical circuits whose core is the ascending arousal system (AAS) (Lee and Dan, 2012). Arising from essential centers in the brainstem, the AAS gives rise to diffuse projections to the thalamus, basal forebrain, basal ganglia, hypothalamus, and neocortex (Holstege and Kuypers, 1987; Jones and Yang, 1985) that regulate both physiological and cognitive functions, including cortical arousal, states of vigilance, sleep-wake cycles, and consciousness (Brown et al., 2011; Flint et al., 2010; Franks, 2008; Jones, 2003; Lee and Dan, 2012; Lydic and Baghdoyan, 2005; Reinoso-Suarez et al., 2011; Xi et al., 1999, 2004).

The neuroscientific and clinical significance of AAS-dependent state regulation is substantial. Pharmacological stimulation of the central thalamus of the AAS has been found to restore consciousness in a minimally conscious patient (Schiff et al., 2007). Likewise, experiments in animals have been successful in reversing the anesthetic state by exogenous stimulation that acts via medial thalamic, basal forebrain, and brainstem components of the AAS (Alkire et al., 2007; Chemali et al., 2012; Fenik et al., 2005; Pillay et al., 2011; Solt et al., 2014). Thus, experimental modulation of the AAS has potential to provide important insight into the regulation of the state of consciousness.

Deep-brain stimulation (DBS) is a powerful clinical therapeutic tool of neuromodulation that has recently emerged as a new focus of functional neuroimaging investigations (Kahan et al., 2014; van Hartevelt et al., 2014). Neuroimaging studies with DBS in animals have focused on neurological conditions, such as epilepsy (Canals et al., 2008; Dunn et al., 2009; Jupp et al., 2006) and Parkinson's disease (Albaugh and Shih, 2014; Lai et al., 2014). Neuroimaging studies of the AAS have been scarce (Edlow et al., 2012; Langsjo et al., 2012) and have not explored the effect of

[1]Department of Anesthesiology, Medical College of Wisconsin, Milwaukee, Wisconsin.
[2]Laboratory of Proteomics, Institute of Biology, Eötvös Loránd University, Budapest. Hungary.

DBS to-date. Thus, it is unclear how activation of the AAS using DBS may alter large-scale networks of the brain, in particular, its functional connectivity (FC) (Lu and Stein, 2013).

To fill this gap of knowledge, in this work, we examined the effect of DBS of the brainstem, a vital region of the AAS, on electrocortical activity and FC. Specifically, we chose to stimulate the oral part of the pontine reticular nucleus (PnO) because it is a central hub for the majority of neurons in the AAS reticular formation with both ascending and descending projections (Jones, 2003; Jones and Yang, 1985; Moruzzi and Magoun, 1949; Watson et al., 2008). We hypothesized that the effect of brainstem stimulation in our model would exert selective effects that primarily involve intrinsic networks associated with the AAS. We chose stimulation parameters that would produce electrocortical desynchronization but no behavioral response at a moderate depth of anesthesia associated with unconsciousness. As we show, PnO stimulation produced cortical desynchronization and an increase in FC within components of the paralimbic circuitry. These results highlight the significance of intrinsic paralimbic FC in states of cortical arousal and help better understand the neuronal mechanism underlying the anesthetic modulation of the state of consciousness and its potential reversibility by DBS in neurological patients (Brown et al., 2010; Schiff, 2012).

Materials and Methods

Animals

All experimental procedures and protocols were approved by the Institutional Animal Care and Use Committee of the Medical College of Wisconsin (Milwaukee, WI). All procedures conformed to the Guiding Principles in the Care and Use of Animals of the American Physiologic Society and were in accordance with the Guide for the Care and Use of Laboratory Animals (National Academy Press, Washington, DC, 1996).

Experiments were performed on nine, naive, adult (280–350 g), male Sprague–Dawley rats (Harlan Laboratories). All animals were housed in a reverse light-dark cycle, in order to eliminate the confounding effects of increased sleep pressure during the experiment, room for at least 10 days prior to surgical implantation. Food and water access was *ad libitum*.

Surgical preparation

The surgical protocol was performed on the day of each experiment. Isoflurane (1.9% ± 0.2%)—distributed via a gas anesthesia mask (Model 929-B Rat Gas Anesthesia Head Holder; David Kopf Instruments, Tujunga, CA), vaporized into a mixture of 30% O_2 and 70% N_2, and delivered at a flow rate of 5 L/min—was used for maintenance during surgery. Core body temperature was rectally monitored (model 73A; YSI, Yellow Springs, OH) and maintained at 37°C with a thermostat-controlled, electric (TC-1000; CWE, Inc., Ardmore, PA) heating pad.

For electrode implantation, sterile, 0.5% bupivacaine was administered subcutaneously for local anesthesia, and the cranium was revealed by laterally reflecting skin and connective tissue. To maintain adequate MR-image quality, hydrogen peroxide and/or a cautery were used to minimize bleeding. To verify the depth of anesthesia, commercially available MR-compatible, Teflon-coated, bipolar platinum-iridium electrodes (Plastics One, Inc., Roanoke, VA), whose tips (~1 mm) were stripped of any Teflon insulation and bent at a 45°, were implanted through burr holes, created using an electric drill, in the cranium. All electrodes were manually inserted over the left frontal cortex (AP = +4.0 and 6.1, $L = -2.34$) such that each wire ''hooked'' underneath the cranium and rested on the surface of the dura. To secure the wires in place, commercially available cyanoacrylate adhesive (Krazy Glue, Columbus, OH), used due to preliminary experiments that indicated minimal adhesive-induced artifact, was applied around the electrode and burr hole. Electroencephalogram (EEG) signal was verified prior to permanently affixing, with orthodontic resin, the recording electrode in place.

In addition to the recording electrode, a homemade, high-impedance, carbon fiber electrode was used to stimulate the PnO (AP = −8.00, $L = -1.3$, angle = 15°, and lowered to a depth such that the middle of the two poles resided at −8.60) as illustrated in Figure 1A and B. Another burr hole, for the placement of a nylon screw (to further anchor the electrode assembly to the cranium), was made ~3-mm anterior to the stimulating electrode site. Orthodontic resin (DENTSPLY Caulk, Milford, DE) was then applied on the left cranium to create one unit (recording electrodes, nylon screw, and stimulating electrode). To minimize the gradient-induced artifact on the EEG, the remaining portion of the platinum recording electrode wires was further insulated using methyl-methacrylate-based orthodontic resin to minimize the circuit loop area through which noise induced by time-varying magnetic fields could be introduced, to provide greater rigidity in order to reduce vibrations in the lead wires (Vasios et al., 2006), and due to its dielectric properties (Breschi et al., 2012; Park et al., 2007; Sword et al., 2008; Tomar et al., 2012; Van Landuyt et al., 2007). The platinum electrodes were then subsequently bent 90° such that the pedestal lay parallel to the dorsal surface of the head. Cyanoacrylate adhesive was then used to seal the surgical site. The recording and stimulating electrode locations are depicted in Figure 1A.

The animal was then transferred to a heated surgical table. The right femoral artery was cannulated with PE-50 polyethylene tubing (Becton-Dickinson, Sparks, MD), flushed previously with heparinized saline, for arterial blood pressure monitoring.

Glass-coated carbon fiber electrode construction

Using of the platinum-iridium electrodes to stimulate the PnO was not feasible because of the significant artifacts due to a mismatch between the magnetic susceptibility of brain tissue and the electrodes. Therefore, we used novel, homemade, MR-compatible, carbon fiber electrodes to stimulate the PnO that did not disturb image quality to the same degree as platinum-iridium electrodes. Bipolar carbon fiber electrodes were constructed from 20 to 50 individual carbon fibers (8-μm diameter) densely packed to a bundle of 0.1–0.4-mm diameter. Each bundle was carefully inserted into a 15-cm, standard, single-barrel borosilicate capillary glass (devoid of a microfilament) with outer and inner diameters of 1.5 and 0.86 mm, respectively. Using a standard laboratory

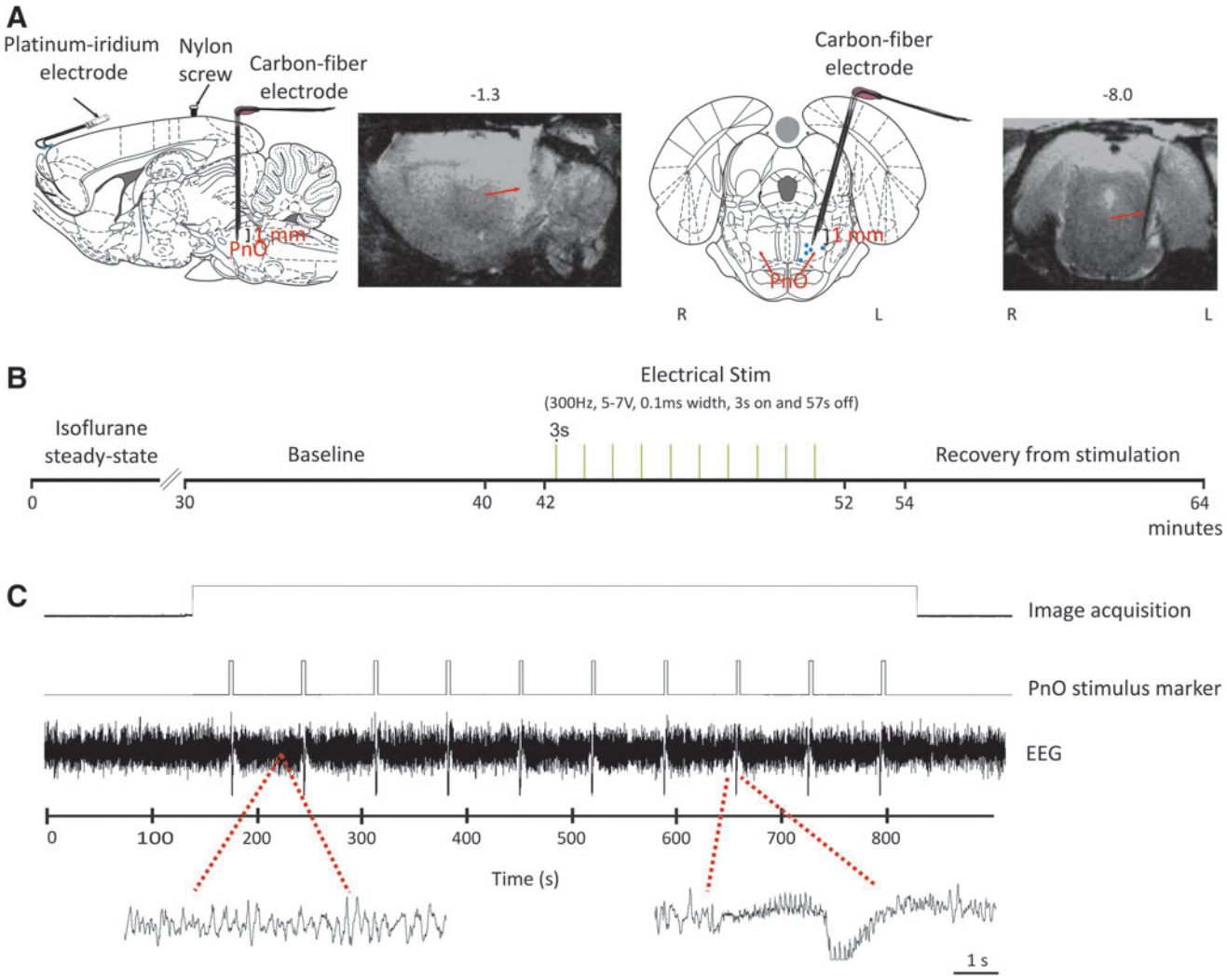

FIG. 1. Schematic of electrode placement and timeline of pontine reticular nucleus (PnO) stimulation. **(A)** Electrode placement overlaid on sagittal and coronal views of the rat brain from the Paxinos rat brain atlas (Paxinos and Watson, 2007). Pairs of platinum-iridium electroencephalogram (EEG) electrodes were placed over the left frontal cortex (AP = +4.0 mm and 6.1 mm, $L = -2.34$ mm) such that each wire ''hooked'' between the cranium and the dura. Carbon fiber stimulating electrode was placed in the PnO (AP = −8.00 mm, $L = -1.3$ mm, angle = 15°, V = −8.60 mm below bregma at the midpoint of the electrode contacts). A nylon screw was used to anchor the electrode assembly in place. Electrode location was confirmed by examining sagittal and coronal anatomical images. Histology was also used to confirm electrode location in five rats; blue closed circles indicate the locations of the electrode tip. **(B)** Experiment timeline with three scans: baseline, electrical stimulation, and recovery from stimulation. Electrical stimulation of PnO commenced after an initial 30-sec delay, and followed a block design of 3 sec on and 57 sec off. **(C)** Example EEG trace during image acquisition, before and after PnO stimulation. Gradient-induced artifact was absent (extended EEG trace left). PnO-stimulus-related artifact was transient (extended EEG trace right). The PnO stimulus marker indicates the timing of the stimulation pulses delivered to the electrode.

Bunsen burner, the carbon fiber–borosilicate glass pairing was pulled, resulting in a single structure between 0.2 and 0.6 mm in diameter. The electrode rod was bent, at two locations, at approximately a 90-degree angle with a tapered neck. The tapered neck was necessary to ensure that the final electrode assembly resided flush with the skull surface after insertion. This was important because the gap between the rat's head and the coil needed to be minimized. Two electrodes were attached using cyanoacrylic adhesive. The electrode assembly was then turned upside down such that the neck rested on the surface of a rectangular segment of Teflon. Then, a layer of dental acrylic was applied to the neck of the electrodes to prevent damage to the carbon fiber bundle. The glass beyond the neck of the electrode was gently broken off to reveal the carbon fiber bundle. The exposed bundle was then attached, via silver print adhesive, to an insulated copper wire. The continuity of connection was verified at the end of this attachment process. The placement of the stimulating electrode was verified via high-resolution anatomical images.

Magnetic resonance imaging hardware preparation and physiological monitoring

All functional magnetic resonance imaging (fMRI) data were acquired on a Bruker 9.4T (AVANCE; Bruker,

Billerica, MA) scanner using a Bruker linear transmit coil (T10325) and rodent surface-receiving coil (T9208). After surgical preparation, the animal was transferred to a recirculating-water-pump-outfitted, G-10 fiberglass MR imaging cradle (Meditherm-III; Gaymar Industries, Orchard Park, New York). Rats continued to receive isoflurane via spontaneous breathing of a 70/30 N_2/O_2 gas mixture. The isoflurane gas mixture (assessed by monitoring the inspired and end-tidal O_2, CO_2, and isoflurane) was adjusted according to the physiology of each animal.

The rats' core temperature was monitored, with a rectal thermometer, and maintained at 37°C ± 0.5°C by a water-pump-driven temperature regulator (Meditherm III; Gaymar Industries). A small animal monitoring system (Model 1025; SA Instruments, Stony Brook, NY) was used to monitor blood pressure, core temperature, and respiratory rate. Pulse oximetry (8600 V; Nonin Medical, Plymouth, MN), inspired/expired O_2 and CO_2 (POET IQ2; Criticare Systems, Waukesha, WI), and heart rate were also acquired. All physiological variables were kept close to normative levels throughout the duration of the experiment protocol, and acquired using WINDAQ software (DATAQ Instruments, Akron, OH).

fMRI protocol

All rats retained the ability to breathe spontaneously throughout the experiment. Of interest was the isoflurane concentration around which loss of consciousness (LOC) was achieved. From previous work it was determined that rats lost their righting reflex between 0.7% and 1.2% isoflurane (Imas et al., 2005). The point at which the loss of righting reflex (LORR), a surrogate measure of unconsciousness in rats, is achieved typically coincides with the presence of slow, delta-dominated EEG waveforms (Franks, 2008). Therefore, the isoflurane concentration was adjusted for each rat so that testing was done at or near LORR, as determined by the presence of slow-wave activity on the recorded EEG (Brown et al., 2010; John and Prichep, 2005). Rats were kept between 1.2% and 1.3% isoflurane throughout the experimental protocol. Figure 1B summarizes the timeline of the fMRI study.

Image acquisition began once the rat reached steady state (as confirmed using the EEG signal) at the desired isoflurane concentration. After a localization scan with the FLASH sequence, a relaxation enhancement rapid acquisition (RARE) pulse sequence was applied to acquire the high-resolution anatomical scan as 15 contiguous coronal slices (center of the eighth slice in alignment with animal midline) with the following acquisition parameters: repetition time (TR) of 2500 msec, echo time (TE) of 8 msec, number of averages = 2, RARE factor of 8, field of view of 35×35 mm^2, matrix size of 256×256, and slice thickness of 1 mm. After the high-resolution anatomical scan, a series of functional scans were taken with a single-shot echo-planar imaging sequence. Using the same geometry as that of the anatomy, the scan parameters of each functional resting session were as follows: TR of 2000 msec, TE of 19 msec, single average, 300 repetitions, and matrix size of 96×96. There were three scans total: baseline, stimulation, and recovery from stimulation.

Electrical stimulation was computer controlled and triggered by an initial pulse from the scanner and delivered using a block design of 3 sec on and 57 sec off. Electrical stimulation of the PnO commenced after an initial 30-sec delay from the onset of image acquisition. Electrical stimulation of the PnO consisted of square pulses delivered at 300 Hz, 5–7 V (depending on when EEG desynchronization was elicited), 0.1 msec width, for 10 cycles (S88; Grass Telefactor, Warrick, RI). In a separate group of rats, outside of the scanner, these stimulation parameters induced EEG desynchronization, but no behavioral responses.

EEG acquisition

The MR-compatible, two-channel connector cable was threaded over the electrode pedestal and fed into a standard stimulate/record switching unit (SRS unit; Grass Technologies, West Warwick, RI). The male output cable from this unit was terminated, via another shielded input cable (CAB-21572; Grass Technologies), on a Grass QP511 Quad AC Amplifier (Grass Technologies). The signal was amplified at 20,000 times, analog band-pass filtered at 1–300 Hz, analog notch filtered at 60 Hz, and digitally sampled at 500 Hz using WINDAQ. EEG signal was acquired continuously throughout the experiment and served as a guide when determining whether steady state isoflurane was achieved prior to functional image acquisition.

Histological verification

In addition to using high-resolution anatomical images ($n = 9$), histology ($n = 5$) was also used to confirm the correct placement of the carbon fiber electrode. The rats were cardioperfused with 300 mL of 0.9% saline, followed by 250 mL of 4% paraformaldehyde solution, through the heart ventricle. The brains were harvested and stored in the paraformaldehyde solution for 24 h, and subsequently transferred to 0.01 M phosphate-buffered saline (pH 7.4). The 200-μm-thick coronal brain sections were cut by a vibratome (Vibratome Series 1000; Ted Pella, Inc., Redding, CA). Brain slices were stained with cresyl violet Nissl and imaged, using a Nikon Eclipse E600 (Nikon, Inc, Melville, NY) microscope, to visualize the location of the electrode site.

Data analysis and statistics: EEG

The gradient-induced artifacts in the EEG signal (Logothetis et al., 2001; Niazy et al., 2005; Schmid et al., 2006), caused by the rapidly changing magnetic field, were mitigated by insulation of MR-compatible platinum-iridium electrode wires with dental acrylic and by laying the wires parallel to the rat's body. Insulation of the electrode led to minimal-to-no gradient–induced artifact on the recorded EEG signal (Fig. 1D). PnO electrical stimulation did cause a large, easily identifiable artifact in the recorded EEG. Data during the 3-sec stimulus on period were excluded from analyses. Therefore, EEG analyses were carried out on segments of data immediately before (−14 sec) and after (+14 sec) PnO stimulation. Specifically, in the pre-stim condition, the 14 sec immediately preceding each stimulation was used. In the post-stim condition, the 14 sec immediately after each stimulation was used. During the baseline and recovery from stimulation recordings, the EEG signal was segmented in a similar manner as those from the stimulation condition (10 total segments with each being 14 sec in length). This resulted in a total of 140 sec of data per

condition for each rat. The EEG data were chosen at a consistent time-point across all animals. Power spectra were calculated from segments of EEG data using Welch's spectral estimation method with a 250-point window and 90% overlap. To reduce the impact of spectral leakage, a Hanning window was used. Band powers ($\delta = 1$–4 Hz, $\theta = 5$–7 Hz, $\alpha = 8$–12 Hz, $\beta = 13$–30 Hz, low-gamma L-$\gamma = 30$–50 Hz, and high-gamma H-$\gamma = 70$–140 Hz) were obtained from the spectra by averaging signal power in the respective frequency ranges. Individual band powers were normalized for each rat at every condition; band power at each condition was divided by the power of the respective band across all conditions for each rat. This was then multiplied by the overall power in each respective band. The global average at each power was then used for the ensuing analyses.

Approximate entropy (ApEn) was also calculated, as detailed in other studies (Bruhn et al., 2000; Pincus, 1991), to further characterize the effect of PnO stimulation on cortical EEG. ApEn is a nonlinear measure of the degree of regularity of a signal. Specifically, a highly regular pattern will produce a low ApEn value, and the opposite holds true for irregular signals. It was computed for the same segments used for the power spectra analyses. Our input parameters ($m = 2$ and $r = 0.25$) were similar to those used previously (Bruhn et al., 2000).

The effect of PnO stimulation on EEG band powers was tested with repeated-measures ANOVA, with conditions (baseline, pre-stim, post-stim, and recovery from stimulation) as independent variables, rat as the subject variable, and band powers as response variables.

The effect of PnO stimulation on ApEn was tested with repeated-measures ANOVA, with conditions (pre-stim and post-stim) as independent variables, rat as the subject variable, and ApEn as the response variable.

All EEG data were analyzed using custom scripts in MATLAB version 7.3.0 (MathWorks, Inc., Natick, MA). Statistical analyses were performed using NCSS 2007 (NCSS, Kaysville, UT). The data were tested for normality using the Shapiro-Wilk test, which yielded no reason to reject the normality assumption. All analyses were two-tailed and a $p < 0.05$ served as the criterion for statistical significance. All data are presented as ± standard deviation from the mean.

Data analysis and statistics: fMRI

The Analysis of Functional NeuroImages (AFNI) software package (NIH, Baltimore, MD) was used for data analyses. The anatomical image set of one rat was chosen as a reference template. The registration tool FLIRT within the FSL software package was used to register all rats' fMRI images onto the reference template.

PnO stimulation led to EEG desynchronization that lasted up to 30 sec. For FC analysis, blood-oxygenation-level dependent (BOLD) time series data obtained during the spontaneous and stimulation scans were segmented into ten 30-sec time series and then concatenated (5 min total). Specifically, the 30-sec segments for the post-stim condition were chosen immediately after each stimulation. All fMRI data were slice time difference corrected, detrended, and frequency filtered (0.08 Hz low-pass) before the FC computation.

FC was assessed using seed-based analysis. All animals were registered to the template brain, and seeds were drawn on this template brain. Specifically, each seed was drawn to the anatomical shape of the structures. Eleven seed regions were manually delineated according to the Paxinos rat brain atlas to represent components of major neurofunctional systems. The mesencephalic reticular formation (mRt), nucleus Basalis of Meynert (NBM), and the central medial thalamic nucleus (CM) were chosen as major components of the AAS for their putative role in modulating cortical arousal and state of consciousness (Alkire et al., 2008; Jones, 2003; Laureys, 2005; Laureys et al., 2005). The anterior cingulate (AC), prefrontal cortex (PFC), retrosplenium (Retro), hippocampus (HI), amygdala (Amyg), and caudate putamen (CPu) were chosen for their roles in information maintenance and integration, learning and memory, and self-referential processing (Ma et al., 2002; Raichle et al., 2001; Vincent et al., 2008). The third group of regions consisted of primary motor cortex (M1) and primary sensory cortex (S1) (Alkire et al., 2008; Dean, 1990; Erchova et al., 2002). Most seeds spanned multiple slices, and all, except CM, were bilateral.

To obtain FC values, the averaged preprocessed BOLD signal time course from each seed region was used as reference, and then cross-correlated (Pearson's r) with each voxel preprocessed time course across the whole brain and represented as FC (r-value) maps for individual animals. All r-values in the individual subject map were transformed to Fisher's Z scores that resulted in data that were approximately normally distributed. All z maps were clustered with minimum cluster size of 56 voxels (clusterwise $p < 0.05$, simulated result with AlphaSim command in AFNI). Group FC maps were generated using a one-sample t-test to examine both negative and positive values. Significantly correlated FC was identified using a threshold of $p < 0.05$. Finally, a two-sample t-test was used to compare the baseline and stimulation conditions.

Results

Physiological variables

Systemic physiology was carefully monitored throughout the course of the experiment. Mean arterial blood pressure, heart rate, and peripheral arterial oxygen saturation were within the normal physiological range during the spontaneous and recovery from stimulation conditions (Table 1). The suggested minor alterations in mean arterial blood pressure and heart rate within 3 min after PnO electrical stimulation were not statistically significant.

Table 1. Physiological Variables Before and After PnO Electrical Stimulation

Time	*BP (mmHg)*	*HR (bpm)*	*SPO_2 (%)*	*Temperature (°C)*
Pre-PnO stim	115 ± 14	315 ± 28	91 ± 5	37.2 ± 0.2
1 min post	135 ± 13	350 ± 26	88 ± 3	37.4 ± 0.5
3 min post	122 ± 15	361 ± 21	89 ± 5	37.5 ± 0.4
5 min post	120 ± 17	322 ± 29	92 ± 4	37.3 ± 0.3
10 min post	123 ± 20	327 ± 31	91 ± 6	37.3 ± 0.2

Mean ± SD.
BP, blood pressure; HR, heart rate; PnO, oral part of the pontine reticular nucleus; SPO_2, blood oxygen saturation.

Electrocortical activity before and after PnO stimulation

Figure 1C shows an example of the recorded EEG trace during intermittent PnO stimulation in one rat. The baseline EEG under isoflurane anesthesia was typical to moderate depth of anesthesia; similar to slow-wave sleep, it was dominated by δ and θ waves. This pattern is common in the unconscious sedated condition—a relatively light state compared with surgical anesthesia. As illustrated in the figure, the EEG pattern recorded during image acquisition was essentially free from artifacts. Typically, gradient-induced artifacts can saturate the EEG signal due to the switching gradients; however, our EEG signals were minimally affected presumably because of the rigidity (minimized vibration in the lead wires), insulation, and circuit-loop area reduction provided by encapsulating the electrode wires with a methylmethacrylate-based orthodontic component resin (Breschi et al., 2012; Khaii et al., 2007; Sword et al., 2008; Van Landuyt et al., 2007; Vasios et al., 2006). PnO stimulation produced a transient artifact in the EEG that typically lasted for 2–3 sec. Once the EEG artifact diminished, a marked shift from slow-wave to low-amplitude and high-frequency (i.e., desynchronized) activity was evident in all rats after PnO stimulation. The desynchronization response to PnO stimulation usually persisted for 10–30 sec (Fig. 2A).

To quantify the effect of PnO stimulation on electrocortical activity, we performed power spectral analysis of the EEG before and after stimulation (Fig. 2B). A condition main effect was found for the δ-band $F(3, 156) = 17.48$, $p < 0.0001$, and the θ-band $F(3, 156) = 8.93$, $p < 0.0001$. PnO stimulation reduced δ-band power from $0.050 \pm 0.012\ \mu v^2$ to $0.036 \pm 0.011\ \mu v^2$. A similar suppression of θ-band power from $0.0477 \pm 0.014\ \mu v^2$ to $0.037 \pm 0.012\ \mu v^2$ was also found ($p < 0.05$, T-K test). None of the other band powers were influenced by PnO stimulation. All band powers were similar in the baseline and recovery from stimulation conditions. PnO stimulation did not elicit any concomitant behavioral responses.

As an additional measure of PnO-stimulation-induced electrocortical desynchronization, ApEn was computed pre- and post-stimulation for each rat. As displayed on Figure 2C, ApEn was dependent on condition [$F(1, 140) = 29.75$, $p < 0.0000$)], with an increase from 1.45 ± 0.37 to 1.63 ± 0.32 after PnO stimulation ($p < 0.05$, T-K test).

Effect of PnO stimulation on FC

PnO stimulation elicited mild increases in BOLD activation in the CPu as well as primary and secondary motor cotices. Whole-brain FC before and after PnO stimulation was assessed by correlating the BOLD time courses of the selected seed regions with those of all other voxels across the entire brain. Before stimulation, the left NBM was significantly correlated with the left and right CPu (voxelwise t-test, $p < 0.05$). To determine the effect of PnO stimulation on FC, group fcMRI maps were generated using a two-sample t-test. Despite multiple seed regions exhibiting FC during baseline, we only found significant regional increases in FC with three of the examined seed regions. The most extensive and consistent changes in FC occurred with the NBM seed (Fig. 3B), between the left NBM and CPu, major regions of the paralimbic system, including the medial PFC, AC cortex, HI, Retro, Amyg, and Thal. Smaller significant FC increases were found between the CM and the left NBM, CPu, and Amyg (Fig. 3C). The retrosplenium also shared increased FC with the left CPu and NBM (Fig. 3D). The effect size of PnO stimulation for FC of the NBM seed was expressed by the averaged Fisher Z-values as displayed in Figure 3E for the nine brain regions for which the FC changes were statistically significant according to the two-sample t-test. No arousal-related transient increases in heart rate could account for the changes in FC.

Discussion

The goal of this study was to investigate the FC changes that accompany DBS of the PnO under light steady-state isoflurane anesthesia. An important feature of our study was the simultaneous acquisition of frontal EEG and BOLD signals.

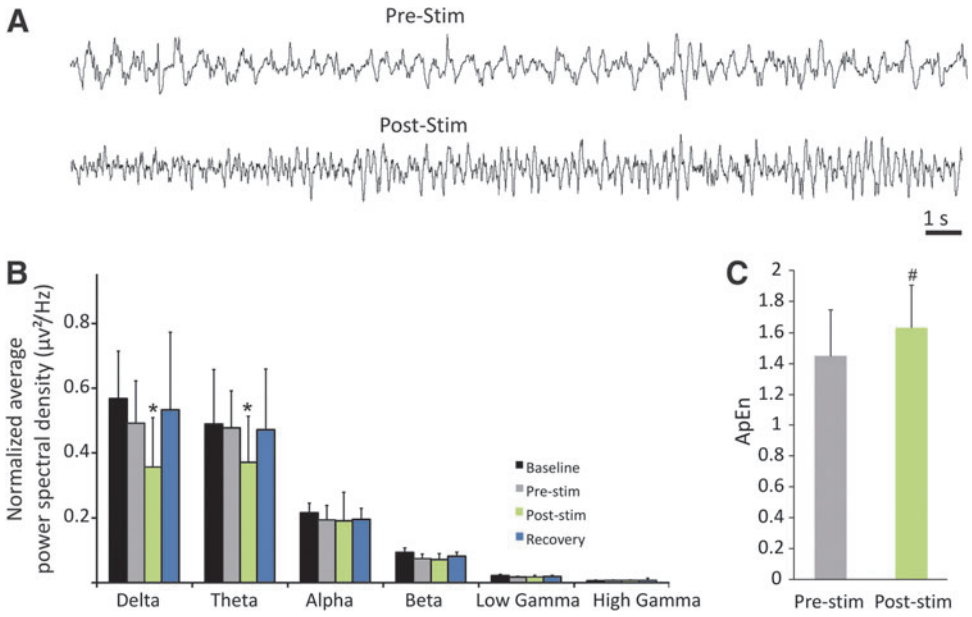

FIG. 2. Electrocortical effect of PnO stimulation. **(A)** EEG traces from a representative experiment. PnO stimulation transforms the EEG from slow wave to a relatively desynchronized pattern. **(B)** Average power spectra from all rats before and after PnO stimulation. PnO stimulation decreases delta and theta power. **(C)** Average approximate entropy (ApEn) from all rats before and after stimulation. PnO stimulation increased ApEn. $^{*}p < 0.05$ versus all other. $^{\#}p < 0.05$ pre-stim versus post-stim. Error bars are ± 1 SD.

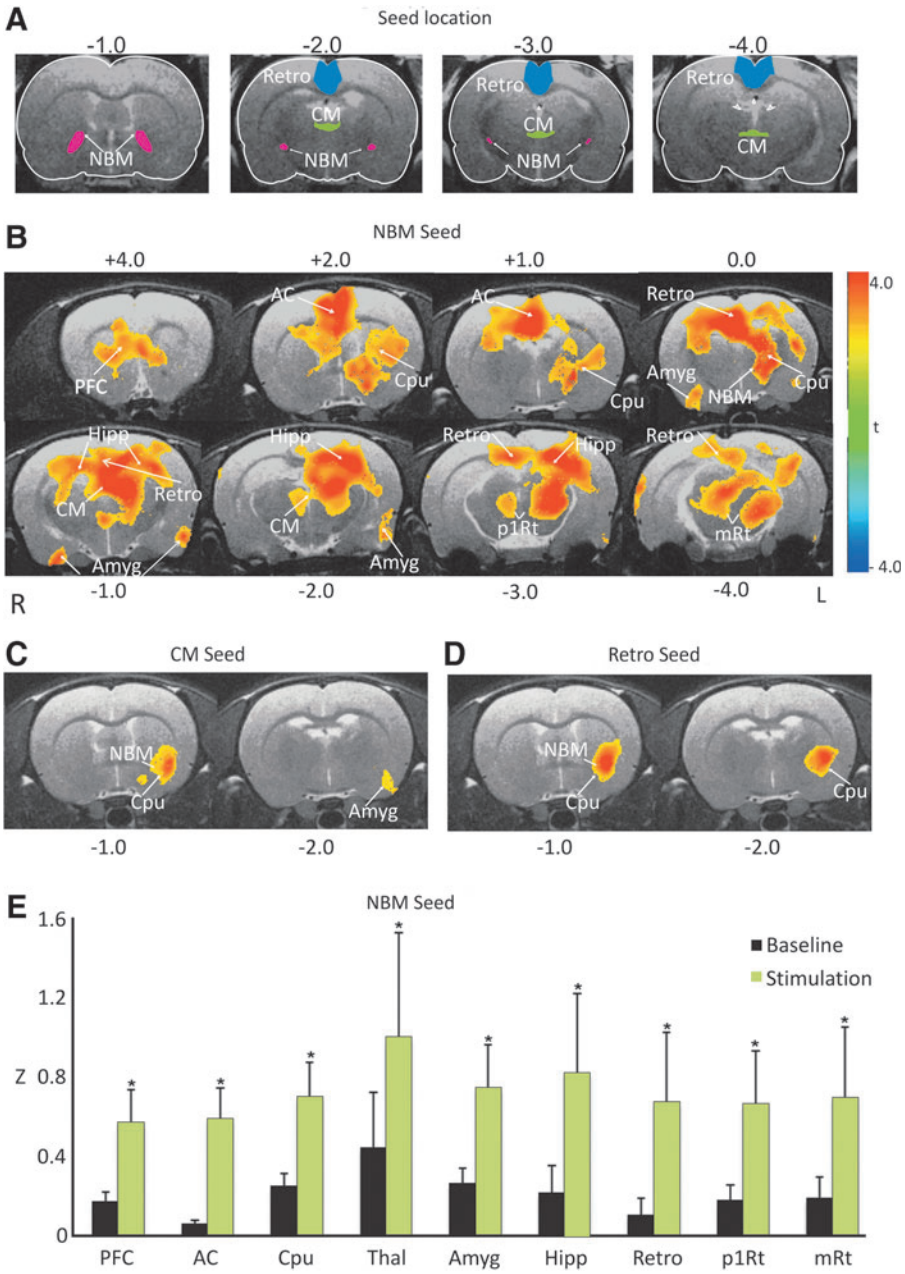

FIG. 3. Effect of PnO stimulation on blood-oxygenation-level-dependent functional connectivity (FC). **(A)** Seed locations for the three that revealed significant regional changes after PnO stimulation. **(B)** Map of significant increases in FC using nucleus Basalis of Meynert (NBM) as seed from voxelwise *t*-test in all animals. Maps are overlaid on sample anatomical images. Color bar indicates *t*-range. Brain regions with significant FC increases ($p < 0.05$) are caudate putamen (Cpu), prefrontal cortex (PFC), anterior cingulate (AC), hippocampus, retrosplenium (Retro), amygdala (Amyg), thalamus (Thal), and reticular formation (p1Rt and mRt). R: right, L: left. **(C)** Map of significant increases in FC using the central medial thalamic nucleus (CM) as seed. **(D)** The same using retrosplenium (Retro) as seed. **(E)** Regional averaged FC values of all animals during baseline (black bars) and after PnO stimulation (green bars), with seed voxels in the left NBM. $*p < 0.05$ versus baseline. Error bars are ± 1 SD. All results are from group data after familywise multiple comparisons.

EEG recording allowed for the continuous monitoring of the state of anesthesia, so that FC could be assessed during a steady state, and the direct assessment of the effect of PnO stimulation on cortical state. We found that PnO stimulation elicited a reduction in δ and θ band power—a clear indication of electrocortical desynchronization. This effect was accompanied by a substantial increase in FC mainly between the left NBM and several regions of the paralimbic network.

DBS is a powerful neuromodulatory therapeutic tool used in the treatment of neurological conditions, such as depression (Mayberg et al., 2005), addiction (Heinze et al., 2009), Parkinson's disease (Fasano et al., 2012; Odekerken et al., 2013), and obsessive compulsive disorder (Figee et al., 2013; Le Jeune et al., 2010). Moreover, there is tremendous potential for DBS-centered therapy in restoring arousal, goal-directed behaviors, communication, and consciousness in patients afflicted with disorders of consciousness (Schiff, 2012). Anesthesia-induced LOC and clinical disorders of consciousness may share common neural mechanisms (Brown et al., 2010). However, unlike traumatic-injury-induced disorders of consciousness, anesthetic agents reversibly alter states of consciousness without disrupting central nervous system integrity (Brown et al., 2010). These properties suggest that DBS-induced recovery of consciousness can be investigated using anesthesia models.

While neuroimaging during DBS in animal models has been primarily confined to epilepsy (Canals et al., 2008; Dunn et al., 2009; Jupp et al., 2006) and Parkinson's disease (Albaugh and Shih, 2014; Lai et al., 2014), their focus was on induced activation rather than FC changes. Further, there are no reports in the neuroimaging literature regarding how FC may be modulated by subcortical centers of the AAS during

altered states of cortical arousal and consciousness. It could be hypothesized that if FC is indeed essential for brain function and even consciousness, then either spontaneous or exogenously generated increases in the tone of the AAS should augment or reorganize the connectivity patterns in relevant functional networks of the brain (Brown et al., 2011; Lee and Dan, 2012; Mashour et al., 2005). This would be particularly expected in sedated or lightly anesthetized states in which cortical response to an increase in AAS activation is plausible (Orth et al., 2006).

A prime candidate for AAS stimulation is the PnO. It exerts comprehensive control over a network of arousal and sleep-wake promoting regions (Jones, 2003; Watson et al., 2008) via its intimate link to subcortical and neocortical structures: the cingulate cortices, HI, diagonal band of Broca, dentate gyrus, locus coeruleus, mamillothalamic tract, preoptic area, medial septal nucleus, NBM, substantia nigra, subthalamic nucleus, and the cerebral cortex (Reinoso-Suarez et al., 2011).

Commensurate with our prior experience (Hudetz et al., 2003; Imas et al., 2005), and similar to that seen in dreamless sleep (Flint et al., 2010), 1.2% isoflurane produced low-frequency, high-amplitude activity EEG (δ- and θ-dominated slow-wave activity) in our rats during the unstimulated state; this has been generally taken as a unitary indication of the unconscious state during which information flow in the brain is impeded (Alkire et al., 2008; Franks, 2008; Le Masson et al., 2002). At this isoflurane concentration, the righting reflex, a widely used behavioral surrogate index of consciousness in rodents (Franks, 2008), is absent.

We used a homemade, high-impedance, MR and biocompatible carbon fiber electrode to stimulate the PnO (Dunn et al., 2009; Jupp et al., 2006; Kitzmiller et al., 2006; Tallgren et al., 2005). As anticipated, electrical stimulation of the PnO induced an attenuation of δ and θ band power, an indication of cortical desynchronization (Jones, 2004; Pillay et al., 2011). A concomitant increase in power at higher frequencies was not observed presumably because the rats continuously received isoflurane anesthesia, and the relatively low intensity of PnO stimulation used did not elicit any behavioral changes. It is possible that higher intensity stimulation may have produced additional EEG changes beyond those observed here. Nevertheless, the suppression of lower frequency power was accompanied by an increase in a nonlinear statistical parameter, ApEn, that measures the amount of regularity in a time-varying signal. In fact, deepening anesthesia has been associated with a decrease in ApEn (Bruhn et al., 2000). The exact relationship between neuroelectrical activity and consciousness remains an area of intense research (Alkire et al., 2008; Hudetz, 2006; Lewis et al., 2012; Mukamel et al., 2014; Murphy et al., 2011; Purdon et al., 2013; Supp et al., 2011).

The DBS-induced electrocortical desynchronization was accompanied by increased FC between several brain regions linked to major subcortical centers of the AAS. In particular, we observed an increase in FC of the left NBM with the CPu, AC, Retro, HI, Thal, and Amyg. This pattern of FC corresponds well with anatomical evidence outlining the extensive reciprocal projections from all brainstem and hypothalamic nuclei that converge on basal forebrain nuclei en route to the HI, limbic structures, and the entire cerebral cortex (Szymusiak, 1995; Zaborszky, 2002; Zaborszky et al., 1991). The basal forebrain region, including the NBM, is the primary source of cholinergic innervation to the cerebral cortex and limbic system (Zaborszky, 2002). Basal-forebrain-mediated cholinergic transmission is a key regulator of rapid eye movement (REM) sleep and wakefulness (Lydic and Baghdoyan, 2005; Vazquez et al., 2002) during which acetylcholine levels in the cortex are high (Everitt and Robbins, 1997; Jasper and Tessier, 1971; Metherate et al., 1992; Perry et al., 1999; Phillis, 2005; Rasmusson et al., 1994), and are suppressed during anesthesia with isoflurane and other agents (Damsma and Fibiger, 1991; Keifer et al., 1994; Ngai et al., 1978; Shichino et al., 1997). Although this has not been tested, the effect of PnO electrical stimulation may have contributed to an assumed increase in acetylcholine release via its projections to the NBM.

In our study, a smaller increase in FC of the CM with the left CPu and NBM was also found. The selection of this nucleus as a seed was in part motivated by previous studies on anesthesia reversal in rodents. Alkire and coworkers (2007) injected nicotine into the CM to elicit spontaneous movement of sevoflurane-anesthetized rats, implying a return of consciousness in the continued presence of the anesthetic. This effect was reproduced by microinjection of a K^+ channel blocking antibody into the CM under both desflurane and sevoflurane anesthesia (Alkire et al., 2009).

The brain networks activated by PnO stimulation included those implicated in the transient recovery of consciousness after exposure to dexmedetomidine or propofol, namely, the brainstem, Thal, AC, hypothalamus, and the limbic core (Langsjo et al., 2012). In fact, forebrain and neocortical dysfunction in severely brain-injured patients may be related to suppression of excitatory neurotransmission from key arousal networks (Schiff, 2010). The increased NBM-paralimbic connectivity may augment effective and episodic information processing in the cortex and in related subcortical networks during wakefulness and REM-like states (Cabeza and Nyberg, 2000; Gardiner, 2001; Hobson, 2009; Louie and Wilson, 2001; Maquet et al., 2000; McDermott et al., 1999; Tulving, 2002; Wiggs et al., 1999). It has also been posited that the paralimbic system may be involved in brain resource allocation via its modulation of attention, awareness, emotional processing, and consciousness (Berridge and Kringelbach, 2008; Kringelbach et al., 2011; Langsjo et al., 2012; Lou et al., 2010, 2011). Similar regions have also been implicated in the emergence from Stage 2 sleep (Balkin et al., 2002) and the occurrence of REM sleep (Miyauchi et al., 2009). Local electrical stimulation, due to its indiscriminant nature, may have induced a transient shift toward a conscious or REM-like state by affecting more than the intended nuclei. In fact, the targeted brainstem region contains numerous distinct nuclei, many of which are affiliated with the reticular activating system (Reinoso-Suarez et al., 2011). A systematic elimination of secondary effects from an activation or deactivation of interacting neuronal groups would require more sophisticated methods, including microinjections or optogenetic manipulations. However, the relatively small electrode tip diameter (0.2–0.6 mm) and the high impedance of the carbon fiber electrode make it unlikely that the stimulation parameters affected an extensive collection of additional brain structures.

While we cannot accurately disentangle the cortical state of the rodent, we speculate that REM-like states may be characterized by conscious experience. While not wakeful, we consider REM sleep a conscious state because it can be

accompanied by subjective experience present during dreaming. Consciousness has been suggested to be a dreaming awake state (Llinas and Pare, 1991). It has been suggested that brain sensory perceptions and imagery during dreaming may be generated and regulated by similar regions to those displaying FC changes in our study (Halgren et al., 1978; Hong et al., 1997; Kreiman et al., 2000).

Somewhat unexpectedly, PnO stimulation did not alter neocortical connectivity, suggesting a possible dissociation with electrocortical desynchronization. However, emergence from anesthesia may be a gradual process with restored network function and connectivity within AAS pathways preceding that of neocortical networks (Langsjo et al., 2012). Although most major brain regions were represented by the selected eleven seeds, the use of additional seeds could reveal heretofore unrecognized changes in connectivity. Perhaps cortical BOLD activation and FC changes are dependent upon the chosen stimulation parameters (Lai et al., 2014). It is also possible that networks shared between the brainstem and neocortex may be especially sensitive to the trauma of surgery, perhaps warranting a more chronic experimental design. Also, the EEG recording was limited to the frontal region, although it is likely that the frontal EEG reflected a fairly general pattern of activation across the cortical mantle (Purdon et al., 2013). It was expected, however, that due to the redundancy of the AAS pathways, local stimulation of the PnO alone would not reactivate all brain systems necessary for a recovery of full wakefulness.

In fact, Sanders and associates (2012) in their three-component consciousness-connectedness-responsiveness model suggest the possibility of a sequential progression of events in the emergence from sleep or anesthesia. Specifically, during emergence, the resumption of internal cognitive processing may occur prior to a reconnection to the environment and the subsequent return of overt behavioral responsiveness. We speculate that the paralimbic activation elicited by PnO stimulation may represent an early step along this sequence, enabling internally generated awareness in the absence of connectedness.

Taken together, we have successfully demonstrated the use of DBS and neuroimaging methods in assessing AAS-stimulation-induced electrocortical desynchronization and associated FC changes during light anesthesia. Specifically, we found an increase in cortical arousal and paralimbic BOLD FC following PnO electrical stimulation. Future work should focus on extensively examining how the induced FC changes are modulated by other anesthetic agents, stimulating other AAS regions, and multiple stimulus parameters. These future investigations should lead to the development of a mechanistic understanding of the induced network effects that accompany DBS-induced restoration of consciousness under anesthesia and in neurologic disorders of consciousness (Schiff, 2012).

Acknowledgments

Research reported in this publication was supported by the National Institute of General Medical Sciences of the National Institutes of Health under Award Numbers R01-GM056398 and R01-EB000215. The content is solely the responsibility of the authors and does not necessarily represent the official views of the National Institutes of Health. The authors thank Dr. Rupeng Li, Department of Biophysics, for his advice with respect to technical aspects of the experiments and to fMRI data analysis.

Author Disclosure Statement

No competing financial interests exist.

References

Albaugh DL, Shih YY. 2014. Neural circuit modulation during deep brain stimulation at the subthalamic nucleus for Parkinson's disease: what have we learned from neuroimaging studies? Brain Connect 4:1–14.

Alkire MT, Asher CD, Franciscus AM, Hahn EL. 2009. Thalamic microinfusion of antibody to a voltage-gated potassium channel restores consciousness during anesthesia. Anesthesiology 110:766–773.

Alkire MT, Hudetz AG, Tononi G. 2008. Consciousness and anesthesia. Science 322:876–880.

Alkire MT, McReynolds JR, Hahn EL, Trivedi AN. 2007. Thalamic microinjection of nicotine reverses sevoflurane-induced loss of righting reflex in the rat. Anesthesiology 107:264–272.

Balkin TJ, Braun AR, Wesensten NJ, Jeffries K, Varga M, Baldwin P, et al. 2002. The process of awakening: a PET study of regional brain activity patterns mediating the re-establishment of alertness and consciousness. Brain 125:2308–2319.

Berridge KC, Kringelbach ML. 2008. Affective neuroscience of pleasure: reward in humans and animals. Psychopharmacology (Berl) 199:457–480.

Breschi M, Fabiani D, Sandrolini L, Colonna M, Sisti L, Vannini M, et al. 2012. Electrical properties of resin monomers used in restorative dentistry. Dent Mater 28:1024–1031.

Bressler SL, Menon V. 2010. Large-scale brain networks in cognition: emerging methods and principles. Trends Cogn Sci 14:277–290.

Brown EN, Lydic R, Schiff ND. 2010. General anesthesia, sleep, and coma. N Engl J Med 363:2638–2650.

Brown EN, Purdon PL, Van Dort CJ. 2011. General anesthesia and altered states of arousal: a systems neuroscience analysis. Annu Rev Neurosci 34:601–628.

Bruhn J, Ropcke H, Hoeft A. 2000. Approximate entropy as an electroencephalographic measure of anesthetic drug effect during desflurane anesthesia. Anesthesiology 92:715–726.

Cabeza R, Nyberg L. 2000. Imaging cognition II: an empirical review of 275 PET and fMRI studies. J Cogn Neurosci 12:1–47.

Canals S, Beyerlein M, Murayama Y, Logothetis NK. 2008. Electric stimulation fMRI of the perforant pathway to the rat hippocampus. Magn Reson Imaging 26:978–986.

Chemali JJ, Van Dort CJ, Brown EN, Solt K. 2012. Active emergence from propofol general anesthesia is induced by methylphenidate. Anesthesiology 116:998–1005.

Damsma G, Fibiger HC. 1991. The effects of anaesthesia and hypothermia on interstitial concentrations of acetylcholine and choline in rat striatum. Life Sci 48:2469–2474.

Dean P. 1990. Sensory cortex: visual perceptual functions. In: Kolb B and Tees RC (eds.) *The Cerebral Cortex of the Rat*. Cambridge: MIT Press: pp. 275–307.

Dunn JF, Tuor UI, Kmech J, Young NA, Henderson AK, Jackson JC, et al. 2009. Functional brain mapping at 9.4T using a new MRI-compatible electrode chronically implanted in rats. Magn Reson Med 61:222–228.

Edlow BL, Takahashi E, Wu ON, Benner T, Dai GP, Bu LH, et al. 2012. Neuroanatomic connectivity of the human

ascending arousal system critical to consciousness and its disorders. J Neuropathol Exp Neurol 71:531–546.
Erchova IA, Lebedev MA, Diamond ME. 2002. Somatosensory cortical neuronal population activity across states of anaesthesia. Eur J Neurosci 15:744–752.
Everitt BJ, Robbins TW. 1997. Central cholinergic systems and cognition. Annu Rev Psychol 48:649–684.
Fasano A, Daniele A, Albanese A. 2012. Treatment of motor and non-motor features of Parkinson's disease with deep brain stimulation. Lancet Neurol 11:429–442.
Fenik VB, Ogawa H, Davies RO, Kubin L. 2005. Carbachol injections into the ventral pontine reticular formation activate locus coeruleus cells in urethane-anesthetized rats. Sleep 28:551–559.
Figee M, Luigjes J, Smolders R, Valencia-Alfonso CE, van Wingen G, de Kwaasteniet B, et al. 2013. Deep brain stimulation restores frontostriatal network activity in obsessive-compulsive disorder. Nat Neurosci 16:386–387.
Flint RR, Chang T, Lydic R, Baghdoyan HA. 2010. GABA(A) receptors in the pontine reticular formation of C57BL/6J mouse modulate neurochemical, electrographic, and behavioral phenotypes of wakefulness. J Neurosci 30:12301–12309.
Franks NP. 2008. General anaesthesia: from molecular targets to neuronal pathways of sleep and arousal. Nat Rev Neurosci 9:370–386.
Gardiner JM. 2001. Episodic memory and autonoetic consciousness: a first-person approach. Philos Trans R Soc Lond B Biol Sci 356:1351–1361.
Halgren E, Walter RD, Cherlow DG, Crandall PH. 1978. Mental phenomena evoked by electrical stimulation of the human hippocampal formation and amygdala. Brain 101:83–117.
Heinze HJ, Heldmann M, Voges J, Hinrichs H, Marco-Pallares J, Hopf JM, et al. 2009. Counteracting incentive sensitization in severe alcohol dependence using deep brain stimulation of the nucleus accumbens: clinical and basic science aspects. Front Hum Neurosci 3:22.
Hobson JA. 2009. REM sleep and dreaming: towards a theory of protoconsciousness. Nat Rev Neurosci 10:803–813.
Holstege JC, Kuypers HG. 1987. Brainstem projections to spinal motoneurons: an update. Neuroscience 23:809–821.
Hong CC, Potkin SG, Antrobus JS, Dow BM, Callaghan GM, Gillin JC. 1997. REM sleep eye movement counts correlate with visual imagery in dreaming: a pilot study. Psychophysiology 34:377–381.
Hudetz AG. 2006. Suppressing consciousness: mechanisms of general anesthesia. Semin Anesth Perioper Med Pain 25: 196–204.
Hudetz AG, Wood JD, Kampine JP. 2003. Cholinergic reversal of isoflurane anesthesia in rats as measured by cross-approximate entropy of the electroencephalogram. Anesthesiology 99: 1125–1131.
Imas OA, Ropella KM, Ward BD, Wood JD, Hudetz AG. 2005. Volatile anesthetics enhance flash-induced gamma oscillations in rat visual cortex. Anesthesiology 102:937–947.
Jasper HH, Tessier J. 1971. Acetylcholine liberation from cerebral cortex during paradoxical (REM) sleep. Science 172: 601–602.
John ER, Prichep LS. 2005. The anesthetic cascade: a theory of how anesthesia suppresses consciousness. Anesthesiology 102:447–471.
Jones B. 2003. Arousal systems. Front Biosci 8:s438–s451.
Jones B, Yang TZ. 1985. The efferent projections from the reticular formation and the locus coeruleus studied by anterograde and retrograde axonal transport in the rat. J Comp Neurol 242:56–92.
Jones BE. 2004. Activity, modulation and role of basal forebrain cholinergic neurons innervating the cerebral cortex. Prog Brain Res 145:157–169.
Jupp B, Williams JP, Tesiram YA, Vosmansky M, O'Brien TJ. 2006. MRI compatible electrodes for the induction of amygdala kindling in rats. J Neurosci Methods 155:72–76.
Kahan J, Urner M, Moran R, Flandin G, Marreiros A, Mancini L, et al. 2014. Resting state functional MRI in Parkinson's disease: the impact of deep brain stimulation on 'effective' connectivity. Brain 137:1130–1144.
Keifer JC, Baghdoyan HA, Becker L, Lydic R. 1994. Halothane decreases pontine acetylcholine release and increases EEG spindles. Neuroreport 5:577–580.
Khaii FLA, Sivagurunathan P, Kamil SRM, Mehrotra SC. 2007. Dielectric studies of methyl methacrylate and butyl methacrylate with primary alcohols using time domain reflectometry. Indian J Pure Appl Phys 45:754–758.
Kitzmiller J, Beversdorf D, Hansford D. 2006. Fabrication and testing of microelectrodes for small-field cortical surface recordings. Biomed Microdevices 8:81–85.
Kreiman G, Koch C, Fried I. 2000. Imagery neurons in the human brain. Nature 408:357–361.
Kringelbach ML, Green AL, Aziz TZ. 2011. Balancing the brain: resting state networks and deep brain stimulation. Front Integr Neurosci 5:8.
Lai HY, Younce JR, Albaugh DL, Kao YCJ, Shih YYI. 2014. Functional MRI reveals frequency-dependent responses during deep brain stimulation at the subthalamic nucleus or internal globus pallidus. Neuroimage 84:11–18.
Langsjo JW, Alkire MT, Kaskinoro K, Hayama H, Maksimow A, Kaisti KK, et al. 2012. Returning from oblivion: imaging the neural core of consciousness. J Neurosci 32:4935–4943.
Laureys S. 2005. The neural correlate of (un)awareness: lessons from the vegetative state. Trends Cogn Sci 9:556–559.
Laureys S, Perrin F, Schnakers C, Boly M, Majerus S. 2005. Residual cognitive function in comatose, vegetative and minimally conscious states. Curr Opin Neurol 18:726–733.
Le Jeune F, Verin M, N'Diaye K, Drapier D, Leray E, Du Montcel ST, et al. 2010. Decrease of prefrontal metabolism after subthalamic stimulation in obsessive-compulsive disorder: a positron emission tomography study. Biol Psychiatry 68:1016–1022.
Le Masson G, Renaud-Le Masson S, Debay D, Bal T. 2002. Feedback inhibition controls spike transfer in hybrid thalamic circuits. Nature 417:854–858.
Lee SH, Dan Y. 2012. Neuromodulation of brain states. Neuron 76:209–222.
Lewis LD, Weiner VS, Mukamel EA, Donoghue JA, Eskandar EN, Madsen JR, et al. 2012. Rapid fragmentation of neuronal networks at the onset of propofol-induced unconsciousness. Proc Natl Acad Sci U S A 109:E3377–E3386.
Llinas RR, Pare D. 1991. Of dreaming and wakefulness. Neuroscience 44:521–535.
Logothetis NK, Pauls J, Augath M, Trinath T, Oeltermann A. 2001. Neurophysiological investigation of the basis of the fMRI signal. Nature 412:150–157.
Lou HC, Gross J, Biermann-Ruben K, Kjaer TW, Schnitzler A. 2010. Coherence in consciousness: paralimbic gamma synchrony of self-reference links conscious experiences. Hum Brain Mapp 31:185–192.
Lou HC, Joensson M, Kringelbach ML. 2011. Yoga lessons for consciousness research: a paralimbic network balancing brain resource allocation. Front Psychol 2:366.

Louie K, Wilson MA. 2001. Temporally structured replay of awake hippocampal ensemble activity during rapid eye movement sleep. Neuron 29:145–156.

Lu H, Stein EA. 2013. Resting state functional connectivity: its physiological basis and application in neuropharmacology. Neuropharmacology 84:79–89.

Lydic R, Baghdoyan HA. 2005. Sleep, anesthesiology, and the neurobiology of arousal state control. Anesthesiology 103: 1268–1295.

Ma J, Shen B, Stewart LS, Herrick IA, Leung LS. 2002. The septohippocampal system participates in general anesthesia. J Neurosci 22:RC200.

Maquet P, Laureys S, Peigneux P, Fuchs S, Petiau C, Phillips C, et al. 2000. Experience-dependent changes in cerebral activation during human REM sleep. Nat Neurosci 3:831–836.

Mashour GA, Forman SA, Campagna JA. 2005. Mechanisms of general anesthesia: from molecules to mind. Best Pract Res Clin Anaesthesiol 19:349–364.

Mayberg HS, Lozano AM, Voon V, McNeely HE, Seminowicz D, Hamani C, et al. 2005. Deep brain stimulation for treatment-resistant depression. Neuron 45:651–660.

McDermott KB, Ojemann JG, Petersen SE, Ollinger JM, Snyder AZ, Akbudak E, et al. 1999. Direct comparison of episodic encoding and retrieval of words: an event-related fMRI study. Memory 7:661–678.

Metherate R, Cox CL, Ashe JH. 1992. Cellular bases of neocortical activation: modulation of neural oscillations by the nucleus basalis and endogenous acetylcholine. J Neurosci 12:4701–4711.

Miyauchi S, Misaki M, Kan S, Fukunaga T, Koike T. 2009. Human brain activity time-locked to rapid eye movements during REM sleep. Exp Brain Res 192:657–667.

Moruzzi G, Magoun HW. 1949. Brain stem reticular formation and activation of the EEG. Electroencephalogr Clin Neurophysiol 1:455–473.

Mukamel EA, Pirondini E, Babadi B, Wong KFK, Pierce ET, Harrell PG, et al. 2014. A transition in brain state during propofol-induced unconsciousness. J Neurosci 34:839–845.

Murphy M, Bruno MA, Riedner BA, Boveroux P, Noirhomme Q, Landsness EC, et al. 2011. Propofol anesthesia and sleep: a high-density EEG study. Sleep 34:283–291A.

Ngai SH, Cheney DL, Finck AD. 1978. Acetylcholine concentrations and turnover in rat brain structures during anesthesia with halothane, enflurane, and ketamine. Anesthesiology 48:4–10.

Niazy RK, Beckmann CF, Iannetti GD, Brady JM, Smith SM. 2005. Removal of fMRI environment artifacts from EEG data using optimal basis sets. Neuroimage 28:720–737.

Odekerken VJJ, van Laar T, Staal MJ, Mosch A, Hoffmann CFE, Nijssen PCG, et al. 2013. Subthalamic nucleus versus globus pallidus bilateral deep brain stimulation for advanced Parkinson's disease (NSTAPS study): a randomised controlled trial. Lancet Neurol 12:37–44.

Orth M, Bravo E, Barter L, Carstens E, Antognini JF. 2006. The differential effects of halothane and isoflurane on electroencephalographic responses to electrical microstimulation of the reticular formation. Anesth Analg 102:1709–1714.

Park JH, Hwang DK, Lee J, Im S, Kim E. 2007. Studies on poly(methyl methacrylate) dielectric layer for field effect transistor: influence of polymer tacticity. Thin Solid Films 515: 4041–4044.

Paxinos G, Watson C. 2007. *The Rat Brain in Stereotaxic Coordinates*. Amsterdam: Academic Press.

Perry E, Walker M, Grace J, Perry R. 1999. Acetylcholine in mind: a neurotransmitter correlate of consciousness? Trends Neurosci 22:273–280.

Phillis JW. 2005. Acetylcholine release from the central nervous system: a 50-year retrospective. Crit Rev Neurobiol 17:161–217.

Pillay S, Vizuete JA, McCallum JB, Hudetz AG. 2011. Norepinephrine infusion into nucleus basalis elicits microarousal in desflurane-anesthetized rats. Anesthesiology 115:733–742.

Pincus SM. 1991. Approximate entropy as a measure of system complexity. Proc Natl Acad Sci U S A 88:2297–2301.

Purdon PL, Pierce ET, Mukamel EA, Prerau MJ, Walsh JL, Wong KFK, et al. 2013. Electroencephalogram signatures of loss and recovery of consciousness from propofol. Proc Natl Acad Sci U S A 110:E1142–E1151.

Raichle ME, MacLeod AM, Snyder AZ, Powers WJ, Gusnard DA, Shulman GL. 2001. A default mode of brain function. Proc Natl Acad Sci U S A 98:676–682.

Rasmusson DD, Clow K, Szerb JC. 1994. Modification of neocortical acetylcholine release and electroencephalogram desynchronization due to brainstem stimulation by drugs applied to the basal forebrain. Neuroscience 60:665–677.

Reinoso-Suarez F, de Andres I, Garzon M. 2011. Functional anatomy of the sleep-wakefulness cycle: wakefulness. Adv Anat Embryol Cell Biol 208:1–128.

Sanders RD, Tononi G, Laureys S, Sleigh JW. 2012. Unresponsiveness not equal unconsciousness. Anesthesiology 116:946–959.

Schiff ND. 2010. Recovery of consciousness after brain injury: a mesocircuit hypothesis. Trends Neurosci 33:1–9.

Schiff ND. 2012. Moving toward a generalizable application of central thalamic deep brain stimulation for support of forebrain arousal regulation in the severely injured brain. Ann N Y Acad Sci 1265:56–68.

Schiff ND, Giacino JT, Kalmar K, Victor JD, Baker K, Gerber M, et al. 2007. Behavioural improvements with thalamic stimulation after severe traumatic brain injury. Nature 448: 600–603.

Schmid MC, Oeltermann A, Juchem C, Logothetis NK, Smirnakis SM. 2006. Simultaneous EEG and fMRI in the macaque monkey at 4.7 Tesla. Magn Reson Imaging 24:335–342.

Shichino T, Murakawa M, Adachi T, Nakao S, Shinomura T, Kurata J, et al. 1997. Effects of isoflurane on *in vivo* release of acetylcholine in the rat cerebral cortex and striatum. Acta Anaesthesiol Scand 41:1335–1340.

Solt K, Van Dort CJ, Chemali JJ, Taylor NE, Kenny JD, Brown EN. 2014. Electrical stimulation of the ventral tegmental area induces reanimation from general anesthesia. Anesthesiology 121:311–319.

Sporns O. 2014. Contributions and challenges for network models in cognitive neuroscience. Nat Neurosci 17:652–660.

Supp GG, Siegel M, Hipp JF, Engel AK. 2011. Cortical hypersynchrony predicts breakdown of sensory processing during loss of consciousness. Curr Biol 21:1988–1993.

Sword J, Pashley DH, Foulger S, Tay FR, Rodgers R. 2008. Use of electrochemical impedance spectroscopy to evaluate resindentin bonds. J Biomed Mater Res Part B Appl Biomater 84B:468–477.

Szymusiak R. 1995. Magnocellular nuclei of the basal forebrain: substrates of sleep and arousal regulation. Sleep 18:478–500.

Tallgren P, Vanhatalo S, Kaila K, Voipio J. 2005. Evaluation of commercially available electrodes and gels for recording of slow EEG potentials. Clin Neurophysiol 116:799–806.

Tomar AK, Mahendia S, Chahal RP, Kumar S. 2012. Structural and dielectric spectroscopic studies of polyaniline-poly(methyl methacrylate) composite films. Synth Metals 162:820–826.

Tulving E. 2002. Episodic memory: from mind to brain. Annu Rev Psychol 53:1–25.

van Hartevelt TJ, Cabral J, Deco G, Moller A, Green AL, Aziz TZ, et al. 2014. Neural plasticity in human brain connectivity: the effects of long term deep brain stimulation of the subthalamic nucleus in Parkinson's disease. PLos One 9:e86496.

Van Landuyt KL, Snauwaert J, De Munck J, Peurnans M, Yoshida Y, Poitevin A, et al. 2007. Systematic review of the chemical composition of contemporary dental adhesives. Biomaterials 28:3757–3785.

Vasios CE, Angelone LM, Purdon PL, Ahveninen J, Belliveau JW, Bonmassar G. 2006. EEG/(f)MRI measurements at 7 Tesla using a new EEG cap (''InkCap''). Neuroimage 33: 1082–1092.

Vazquez J, Lydic R, Baghdoyan HA. 2002. The nitric oxide synthase inhibitor NG-Nitro-L-arginine increases basal forebrain acetylcholine release during sleep and wakefulness. J Neurosci 22:5597–5605.

Vincent JL, Kahn I, Snyder AZ, Raichle ME, Buckner RL. 2008. Evidence for a frontoparietal control system revealed by intrinsic functional connectivity. J Neurophysiol 100:3328–3342.

Watson CJ, Soto-Calderon H, Lydic R, Baghdoyan HA. 2008. Pontine reticular formation (PnO) administration of hypocretin-1 increases PnO GABA levels and wakefulness. Sleep 31:453–464.

Wiggs CL, Weisberg J, Martin A. 1999. Neural correlates of semantic and episodic memory retrieval. Neuropsychologia 37:103–118.

Xi MC, Morales FR, Chase MH. 1999. Evidence that wakefulness and REM sleep are controlled by a GABAergic pontine mechanism. J Neurophysiol 82:2015–2019.

Xi MC, Morales FR, Chase MH. 2004. Interactions between GABAergic and cholinergic processes in the nucleus pontis oralis: neuronal mechanisms controlling active (rapid eye movement) sleep and wakefulness. J Neurosci 24:10670–10678.

Zaborszky L. 2002. The modular organization of brain systems. Basal forebrain: the last frontier. Prog Brain Res 136:359–372.

Zaborszky L, Cullinan WE, Braun A. 1991. Afferents to basal forebrain cholinergic projection neurons: an update. Adv Exp Med Biol 295:43–100.

Address correspondence to:
Anthony G. Hudetz
Department of Anesthesiology
Medical College of Wisconsin
8701 Watertown Plank Road
Milwaukee, WI 53226

E-mail: ahudetz@mcw.edu